Article

Understanding Fatigue Failure in Binary Rubber Blends: Role of Crack Initiation and Propagation

PAN Lijia[1], WANG Yuge[2,3], WEI Lai[1]✉ and SUN Zhaoyan[1,2,3]✉

Received January 3, 2024
Accepted January 31, 2024

Under cyclic loading conditions, the breakdown of rubber products is mainly caused by the formation and spread of cracks. This study focuses on understanding how cracks initiate and grow during the fatigue failure of blended rubber. We prepared composite materials by blending bio-mimetic rubber (BMR) and butadiene rubber (BR) in different mass ratios and evaluated their resistance to crack initiation and propagation. Our results indicate a clear trend: as the BR content increases, crack initiation in blended rubber is inhibited, while crack propagation is enhanced. This shift leads to a change in the primary factor influencing fatigue fracture from crack initiation to crack propagation. Additionally, we observed that the fatigue life of the rubber blend initially increases and then decreases as the BMR content rises, indicating a critical threshold when the mass ratio of BMR to BR is comparable. By closely examining the materials using a scanning electron microscope (SEM) and image analysis, we confirmed that before the threshold, crack initiation is the dominant factor in fatigue failure, while after the threshold, crack propagation takes over. This study provides valuable insights into the mechanisms behind fatigue failure in rubber blends, contributing to a better understanding of this important material behavior.

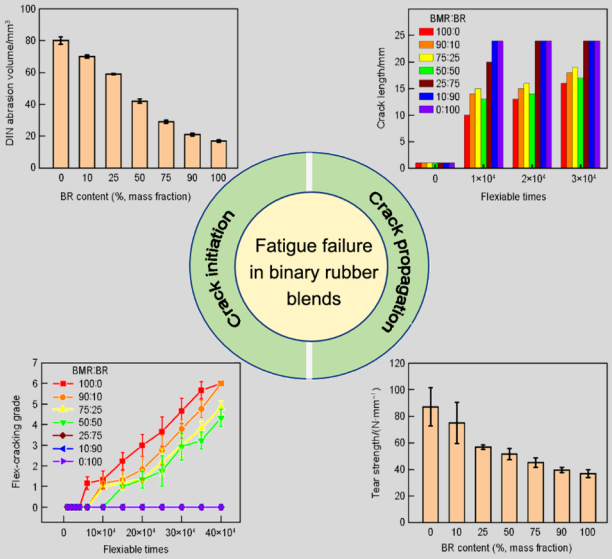

Keywords Blended rubber; Fatigue failure; Crack initiation; Crack propagation; Fracture microstructure

1 Introduction

Rubber, owing to its distinctive viscoelastic properties and impressive mechanical strengths, is widely employed in applications subjected to cyclic loading, including tires, gaskets, and vibration isolators. However, prolonged exposure of rubber products to reciprocating forces can culminate in the initiation and propagation of cracks, ultimately leading to fatigue failure and adversely affecting the service life of these products.[1−8] Despite extensive research, the scholarly community remains divided on identifying the primary factor driving rubber fatigue failure, whether it is crack initiation or crack propagation. Shangguan *et al.*[9] conducted tensile fatigue tests on carbon black-filled natural rubber samples, revealing that crack initiation accounted for over 90% of the total fatigue life, thereby supporting the notion that crack initiation is the primary cause of fatigue failure. This perspective is reinforced by Le Cam *et al.*,[10] who, through scanning electron microscopy (SEM), observed damaged carbon black aggregates within the rubber matrix and near the sample surface, surrounded by numerous cracks. Conversely, Gent *et al.*[11] and Ghosh *et al.*[5] argued for crack growth as the dominant factor in rubber fatigue failure. Gent's investigation demonstrated a consistent crack propagation mechanism in samples with intentional defects and those without, implying direct crack propagation from the defect to fatigue fracture. Ghosh's study on nature rubber/butadiene rubber (NR/BR) blend rubber concluded that fatigue failure ensued not from crack initiation but from the

✉ SUN Zhaoyan
zysun@ciac.ac.cn
✉ WEI Lai
weilai@ylnu.edu.cn
1. Xinjiang Laboratory of Phase Transitions and Microstructures in Condensed Matters, College of Physical Science and Technology, Yili Normal University, Yining 835000, P. R. China;
2. State Key Laboratory of Polymer Physics and Chemistry, Changchun Institute of Applied Chemistry, Chinese Academy of Sciences, Changchun 130022, P. R. China;
3. University of Science and Technology of China, Hefei 230026, P. R. China

https://doi.org/10.1007/s40242-024-4001-0

subsequent propagation of cracks under cyclic loading conditions. The lack of consensus within the academic community underscores the complexity of understanding the intricate mechanisms governing rubber fatigue failure.

Nevertheless, in the case of blended rubber, the influence of crack initiation and propagation on fatigue properties extends beyond the inherent characteristics of the rubber itself and is intricately tied to the blending ratio.[12−17] For instance, Beatty *et al*.[18] conducted comprehensive tensile fatigue tests on NR/BR blends with varying ratios, discovering that the optimal fatigue performance occurred at a balanced 50/50 blending ratio. Numerous scholars have explored the dynamics of crack initiation and propagation in blended rubber with varying blending ratios. Song *et al*.[19] emphasized that an increase in BR content enhances the anti-crack initiation capability of the blend. They attribute this phenomenon to the softer molecular chain structure of BR, resulting in weaker intermolecular forces and reduced internal friction between large molecular chains. Mathew *et al*.[15] substantiated this conclusion by observing the experiment's surface roughness variation during fatigue failure, noting a decrease in roughness and crack initiation with increasing BR content.

In investigations related to crack growth, Chiu *et al*.[20] found a decrease in tear strength for NR/BR mixtures with higher BR content, accompanied by diminished anti-crack growth ability. Ghosh *et al*.,[5] utilizing optical microscopy, observed that samples with high BR content exhibited more regular crack edges and faster crack propagation. Moreover, Kim *et al*.[13] identified fewer crack path branches and lower energy consumption in BR compared to NR, contributing to BR's higher crack propagation rate. This observation is attributed to the weak self-reinforcing properties of BR. Collectively, these studies highlight a trend: an increase in BR content corresponds to heightened resistance to crack initiation and diminished resistance to crack propagation in blended rubber. Despite these findings, the paramount factor in the fatigue failure process remains unclear.

In this study, we delve deeper into understanding the impact of crack initiation and propagation on the fatigue failure of binary blend rubber. Specifically, we explore these effects on bio-mimetic rubber (BMR), a synthetic rubber akin to natural rubber,[21,22] in combination with BR, utilizing wear and flex fatigue tests alongside tear and crack growth tests. Our findings reveal a distinct enhancement in the fatigue performance of blended rubber when the BMR content is comparative to that of BR. However, blends with low BR content exhibit susceptibility to crack initiation, whereas those with high BR content demonstrate vulnerability to crack propagation.

Building upon these observations, we posit that fatigue failure predominantly stems from crack initiation before a critical threshold is reached, subsequently transitioning to a situation where crack propagation becomes the primary mechanism. To further substantiate this conclusion, we employed SEM to observe the fracture morphology of samples following fatigue failure. The analysis indicates that pre-threshold fatigue failure is primarily attributed to crack initiation, as evidenced by a relatively rough and ductile fracture surface. Conversely, post-threshold fatigue failure is mainly associated with crack propagation, characterized by a relatively smooth and brittle fracture morphology. This corroborates and reinforces our initial findings, providing a comprehensive understanding of the nuanced mechanisms governing fatigue failure in blended rubber.

2 Experimental

2.1 Instruments and Materials

SS-RPMS-01 mixer and SS-RPMS-02 open two-roll mill (Dongguan Songshu Testing Instrument Co., Ltd., Dongguan, China); M-3000AU moving die rheometer, Plate vulcanizer and De Mattia flexing machine (Dongguan High-speed Railway Testing Instrument Co., Ltd., Dongguan, China); Z005 testing machine (Zwick, Germany); BPG-9140A Electric thermostatic drying oven (Shanghai Precision Scientific Instrument Co., Ltd., Shanghai, China); deutsche industrie normen (DIN) abrader and Sigma300 ultra-low temperature scanning electron microscope (Carl Zeiss, Germany).

Bio-mimetic rubber (BMR, Mooney viscosity $ML_{1+4}^{100\ ^{\circ}C}$ = 101, polymerization of isoprene as monomer under the condition of rare earth catalyst and additives) was provided by Changchun Institute of Applied Chemistry of Chinese Academy of Sciences (CIAC, China).[23] Polybutadiene rubber (BR, Mooney viscosity $ML_{1+4}^{100\ ^{\circ}C}$=45) was purchased from PetroChina Jilin Petrochemical Co., Ltd. (China). Carbon black N234 was purchased from Shanghai Cabot Chemical Co., Ltd. (China). Zinc oxide was purchased from Jiaxing Beihua Polymer Auxiliary Co., Ltd. (China); stearic acid was purchased from Tianjin Wilmar Oil Technology Co., Ltd. (China). Antioxidant 4010NA (*n*-isopropyl-*N*′-phenyl-*p*-phenylenediamine) was purchased from Tianjin Kemal Chemical Co., Ltd. (China). Sulfur OT-20 was purchased from Shanghai Jinghai Chemical Co., Ltd. Accelerator NS (*N*-*tert*-butyl-2-benzothiazolisulfonamide) was purchased from Nantong Reform Petrochemical Technology Co., Ltd. (China). All reagents used in the experiments were of industrial grade purity, and the experimental formula is detailed in Table 1.

https://doi.org/10.1007/s40242-024-4001-0

Table 1 Recipes of BMR/BR blends ("phr" refers to mass parts per hundred parts rubber)

Ratio of BMR/BR	Recipe/phr							
	BMR	BR	CB	ZnO	Stearic acid	4010NA	NS	Sulfur
100/0	100	0	52	5	2	1.5	0.8	2.2
90/10	90	10	52	5	2	1.5	0.8	2.2
75/25	75	25	52	5	2	1.5	0.8	2.2
50/50	50	50	52	5	2	1.5	0.8	2.2
25/75	25	75	52	5	2	1.5	0.8	2.2
10/90	10	90	52	5	2	1.5	0.8	2.2
0/100	0	100	52	5	2	1.5	0.8	2.2

2.2 Preparation of Rubber Compounds

Various methods exist for preparing mixed rubber, including one-stage mixing, multiple mixing, reverse mixing, and others. In this investigation, a two-stage mixing method was employed to prepare the mixed rubber. In the first stage, the rubber was placed into the mixer for plasticization with 30 s (referred to as mastication time). Following this, zinc oxide, stearic acid, antioxidant, and half of the carbon black were added and mixed for an additional 30 s. Subsequently, the remaining carbon black was introduced, and the mixture underwent further mixing for 5 min. Thus the total mixing time was 5.5 min, and the resulting rubber compound was then extracted. Following a 12-h room temperature storage period, the second stage commenced. The obtained rubber compounds were heated at 75 °C in an oven for 10 min. Subsequently, they were introduced into the mixer operating at 70 °C and 30 r/min. Accelerators and sulfur were added and mixed for 2 min. The compounds were further plasticized and processed on an open two-roll mill at 16 r/min for 5 min, maintaining front and back roller temperatures at 45 and 50 °C, respectively. During this procedure, the rubber mixture underwent three cuts on each side. It should be noted that, changing mastication time or total mixing time does affect the dispersity of fillers in the rubber matrix and the subsequent mechanical properties of rubber materials. To specifically investigate crack initiation and propagation during flex fatigue, we standardized the mastication time and mixing time across all samples analyzed in this research. The vulcanized rubber was prepared using a plate vulcanizer at a pressure of 5000 MPa and a temperature of 145 °C. The vulcanization time was determined using the optimal vulcanization time (TC90)+ 5 min, obtained through testing the vulcanization curve of the compound at 15 MPa and 145 °C with a moving die rheometer.

2.3 Characterization Methods

Tensile fatigue test: a 6-station De Mattia flex testing machine was used for tensile fatigue test. The adjustable fixture spacing ranged from 55 mm to 100 mm, with a test frequency of 5 Hz. Rectangular test samples measuring 100 mm×10 mm×2 mm were utilized, and the distance between standard distance lines was maintained at 40 mm. Six samples were tested under each experimental condition, and the statistical average value of the six samples was calculated. Abrasion test: the abrasion performance of vulcanized rubber was assessed according to GB/T9867-2008, utilizing an abrader. A 10 N force was applied to the cylindrical sample, producing an abrasion stroke on the cylindrical roller spanning 20 m. The roller dimensions were 150 mm in diameter and 500 mm in length, rotating at a speed of 40 r/min. Five samples were tested per experimental condition.

Tear test: the tear strength test was conducted following the GB/T529-2008 "Right-angle Sample Without Cutting Method." The tensile rate was set at 500 mm/min, and the sample thickness was 2 mm. Six specimens were subjected to the tear test, and six splines were cut for each sample.

Flex cracking and crack growth test: flex cracking and crack growth tests were performed in accordance with GB/T13934-2006, utilizing a 6-station De Mattia flexure testing machine. Custom molds were used for sample preparation. For each blending ratio, six independent samples were conducted and the average value of these six independent samples was calculated and recorded. In the flex cracking test, the sample movement speed was 300 r/min, and the flexural number was set at 400000 times. The flex cracking grade was recorded every 10000 times before 50000 times and then every 50000 times until reaching the highest flex cracking grade or 400000 flexural cycles. For the crack growth test, the flex frequency was 300 r/min, the number of flexures was 30000, and the initial crack length was 1 mm. The length of a crack was recorded every 10000 flexures of the sample.

Microstructure: the surface morphology of the compound was observed *via* ultra-low temperature SEM. For samples after the tensile fatigue test, the entire fatigue sample's fracture surface was taken for observation. The

https://doi.org/10.1007/s40242-024-4001-0

section was treated with gold spraying to enhance electrical conductivity. Testing was conducted at a 15 kV acceleration voltage and a 10 mA current.

3 Results and Discussion

To investigate the intricate interplay of crack initiation and propagation in the process of tensile fatigue failure in binary blended rubber, we conducted a comprehensive characterization of the tensile fatigue properties across various blending ratios of BMR/BR blends. To gain a deeper understanding of the impact of crack initiation on fatigue failure, we designed specialized experiments, including abrasion and flex fatigue tests, specifically tailored to assess the blend's resistance to crack initiation.[15,24] Concurrently, the blend's capacity to withstand crack growth was evaluated through tear strength tests and crack growth experiments, shedding light on the nuanced influence of crack growth on fatigue failure.[13,25]

To provide a more direct illustration of the influence of crack initiation and propagation on tensile fatigue failure, we employed SEM to scrutinize the tensile fatigue failure section of the blends. This microscopic examination aimed to reveal the intricate details of crack initiation and propagation, offering valuable insights into the underlying mechanisms governing the fatigue behavior of the BMR/BR blends. The amalgamation of these varied experimental approaches allows for a comprehensive analysis of the multifaceted factors contributing to tensile fatigue failure in binary blended rubber.

3.1 Fatigue Properties of BMR/BR Blend Rubber

The tensile fatigue test serves as a critical measure to assess the strength and durability of rubber materials, offering insights into their performance decrease and eventual fracture under the strain of repeated stretching under real-world conditions.[26,27] Fig. 1 presents the results of the tensile fatigue tests conducted on BMR/BR blends featuring various blending ratios. Notably, the fatigue life of BR surpasses that of BMR, suggesting an intrinsic difference in fatigue resistance between the two components. Generally, an increase in BR content correlates with an improvement in the fatigue life of the blended rubber. However, this improvement follows a discernible non-monotonic pattern. Remarkably, when the BMR and BR contents are closely aligned, the blended rubber exhibits exceptional fatigue properties. Nevertheless, as the BR content continues to rise, the fatigue life of the blend gradually diminishes, approaching the fatigue life of the individual BR component. This trend aligns with findings from previous studies on NR/BR blends.[18]

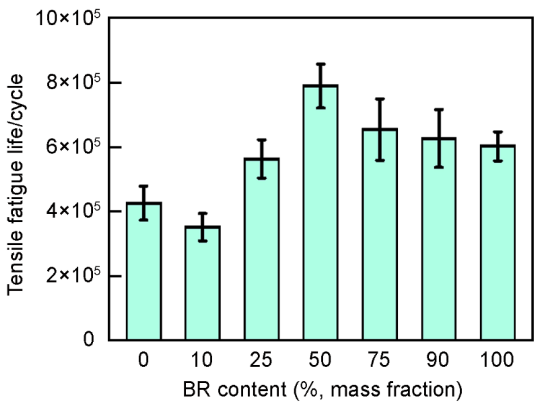

Fig. 1 Tensile fatigue life of vulcanized BMR/BR rubber compounds with different BR contents

Given the established connection between fatigue failure and crack initiation and propagation,[28,29] we sought to delve deeper into the crack characteristics of BMR/BR blends at varying proportions. The observed trends in fatigue life underscore the intricate relationship between blending ratios and the interplay between crack initiation and propagation, offering valuable insights into the fatigue behavior of the blended rubber.

3.2 Crack Initiation in BMR/BR Blends

Abrasion, as a unique fatigue process, induces the formation of cracks on the material surface, signifying an initiation phase without subsequent propagation. Thus, abrasion resistance provides valuable insights into a rubber's ability to withstand crack initiation.[26] Fig. 2A illustrates that the abrasion volume of BMR is approximately four times greater than that of BR. Notably, the abrasion volume undergoes a substantial reduction by about half when the BMR and BR mass ratio is 50/50. The trend of monotonically decreasing abrasion volume in BMR/BR blends with increasing BR content signifies not only an enhancement in abrasion resistance but also an increased resistance to crack initiation in the blends. This observation aligns with the findings of Song *et al.*,[19] who arrived at a similar conclusion in the abrasion study of NR/BR blends.

The existence of C—C single bonds in the BR molecule enables molecular chain rotation around these bonds, reducing friction between molecular chains and enhancing resilience against external forces, thereby lowering the likelihood of crack initiation. This molecular characteristic contributes to the observed improvement in crack initiation resistance with an increase in BR content. The results of flex fatigue tests further corroborate this perspective, as depicted in Fig. 2B. Samples with lower BR content exhibit higher cracking grades under the same cycle conditions, indicating more pronounced crack initiation. Conversely, when the BR content exceeds half, the cracking grade consistently

https://doi.org/10.1007/s40242-024-4001-0

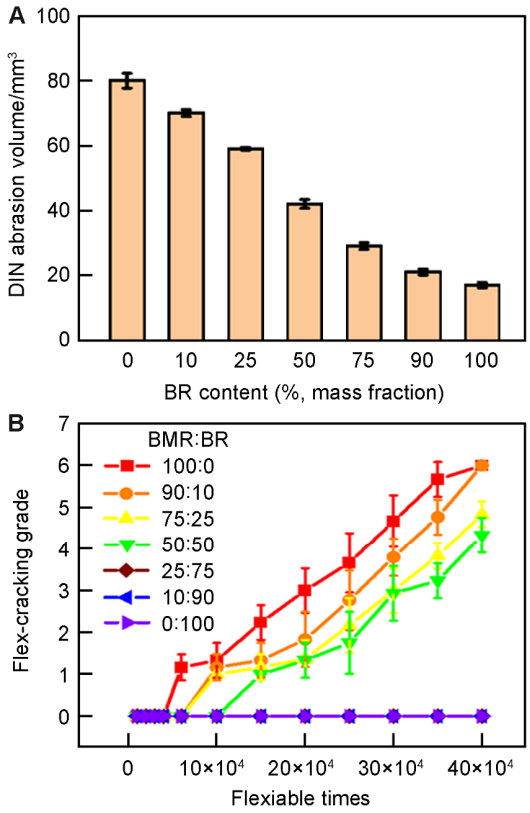

Fig. 2 DIN abrasion volume (A) and cracking grade (B) during flex fatigue of vulcanized BMR/BR rubber compounds with different BR contents

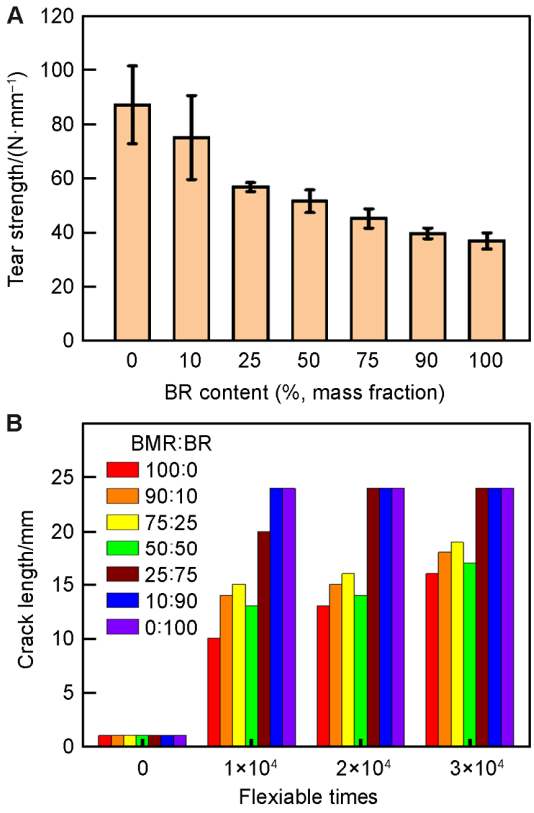

Fig. 3 Tear strength (A) and the crack propagation length (B) during flex fatigue of vulcanized BMR/BR rubber compounds with different BR contents

maintains at grade 0 within the tested cycle range, signifying reduced susceptibility to crack initiation in these blends. This trend aligns with observations made by Mathew *et al*.,[15] who, using SEM on the fractured surfaces of NR/BR blends subjected to flex fatigue, noted increased surface roughness when BR content was low, attributing it to crack initiation.

Collectively, these studies consistently underscore that lower BR content in the blend corresponds to heightened susceptibility to crack initiation, providing additional insights that the primary factor contributing to fatigue failure at this juncture may indeed be crack initiation.

3.3 Crack Propagation in BMR/BR Blends

Tearing, the phenomenon of crack propagation in elastomer materials like rubber under tensile forces, serves as a pivotal aspect for evaluating both tearing resistance and the rubber's capability to resist crack propagation.[25] Fig. 3A reveals that the tear strength of BMR is approximately twice that of BR. However, as the BR content increases in the blend, tear strength gradually diminishes, converging toward the tear strength of a neat BR component. This decline underscores a reduction in the blended rubber's resistance to crack propagation with an escalating BR content. A parallel study on NR/BR blends by Chiu *et al*.[20] aligns with this observation, noting a decrease in tear strength with an increasing proportion of BR, attributed to the weak self-reinforcing nature of BR.

The outcomes of the crack growth experiment, as depicted in Fig. 3B, echo the tear strength findings. Under identical initial crack conditions, the blend exhibits increasing crack dimensions with a rise in cyclic loading times, with higher BR content showcasing a swifter crack propagation rate. When BMR content is comparative with BR, there is a noticeable deceleration in crack propagation, possibly attributable to the bicontinuous structure formed by the blend, which serves to impede the crack propagation rate.[13] Generally, the resistance to crack propagation diminishes with an elevated BR content. A parallel study by Ghosh *et al*.[5] supported this notion, observing through SEM that NR/BR blends with higher BR content exhibited a more regular crack profile and a faster crack growth rate. The authors attributed this to the low crystallinity of BR, impeding the formation of crystals at the crack tip and reducing stress dissipation.

Moreover, Kim *et al*.[13] noted in their investigation that the crack propagation rate of BR surpassed that of NR. They observed fewer branches in the crack propagation path of BR, resulting in lower energy consumption during

https://doi.org/10.1007/s40242-024-4001-0

crack propagation and an accelerated crack propagation rate. These collective findings underscore a substantial increase in the crack propagation rate of the blend with higher BR content, indicating a diminished capacity to resist crack propagation. This suggests that fatigue failure at this stage may be primarily driven by crack propagation.

3.4 Microstructure Analysis

To substantiate the discernible shift in the leading factors driving fatigue failure before and after the threshold, a clearer observation of the tensile fatigue samples was conducted using SEM. The comprehensive topography in Fig. 4 reveals that fractures occurring before the threshold predominantly exhibit rough areas, a characteristic associated with crack initiation, as suggested by previous studies.[15] This indicates the susceptibility of the sample to microscopic crack formation under cyclic loading, resulting in a ductile fracture section. Moreover, the local magnifications corresponding to Fig. 5, A and B unveil an abundance of cracks and distinctive void structures, including spherical aggregates or "cavitations".[17] This further supports the conclusion that pre-threshold tensile fatigue failure is primarily governed by crack initiation at the microscopic level.

As observed in Fig. 4, an increase in BR content in the blend correlates with a gradual shift toward a smoother fracture surface, indicative of brittle fracture. Research suggests that a smooth surface implies resistance to crack formation under cyclic load, but once initiated, cracks propagate rapidly.[20] The locally enlarged images corresponding to D and E in Fig. 5 reveal that post-threshold fractures exhibit reduced spherical aggregates and pores, weakening the nano-cavitation phenomenon and indicating a decreased likelihood of microdefects. However, the crack growth edge appears more regular, with sharper crack tips than the initiation points, reflecting an accelerated crack propagation rate.[5,7] This reinforces the conclusion that tensile fatigue failure after the threshold is predominantly driven by crack propagation.

A comprehensive SEM analysis elucidates a transition in the tensile fatigue section of BMR/BR blend from ductile

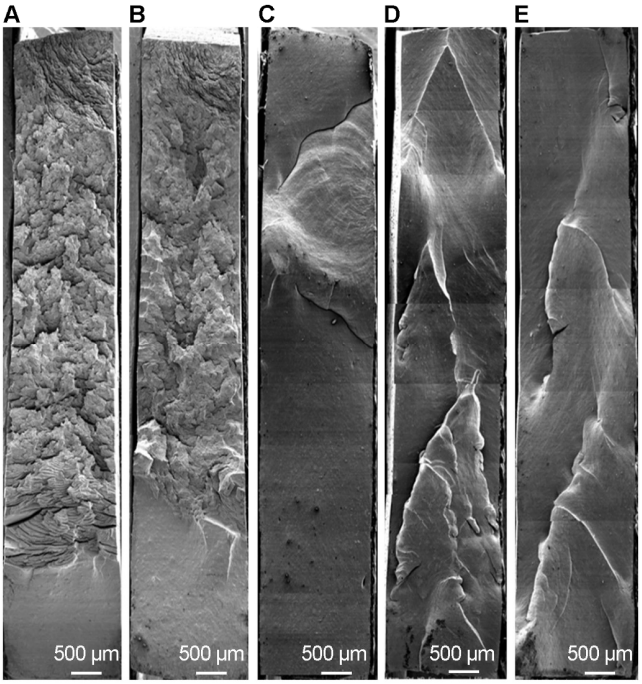

Fig. 4 SEM images of whole section of fatigue sample at low magnification

Their blending ratios from A to E are BMR/BR (100/0), BMR/BR (90/10), BMR/BR (50/50), BMR/BR (10/90) and BMR/BR (0/100), respectively.

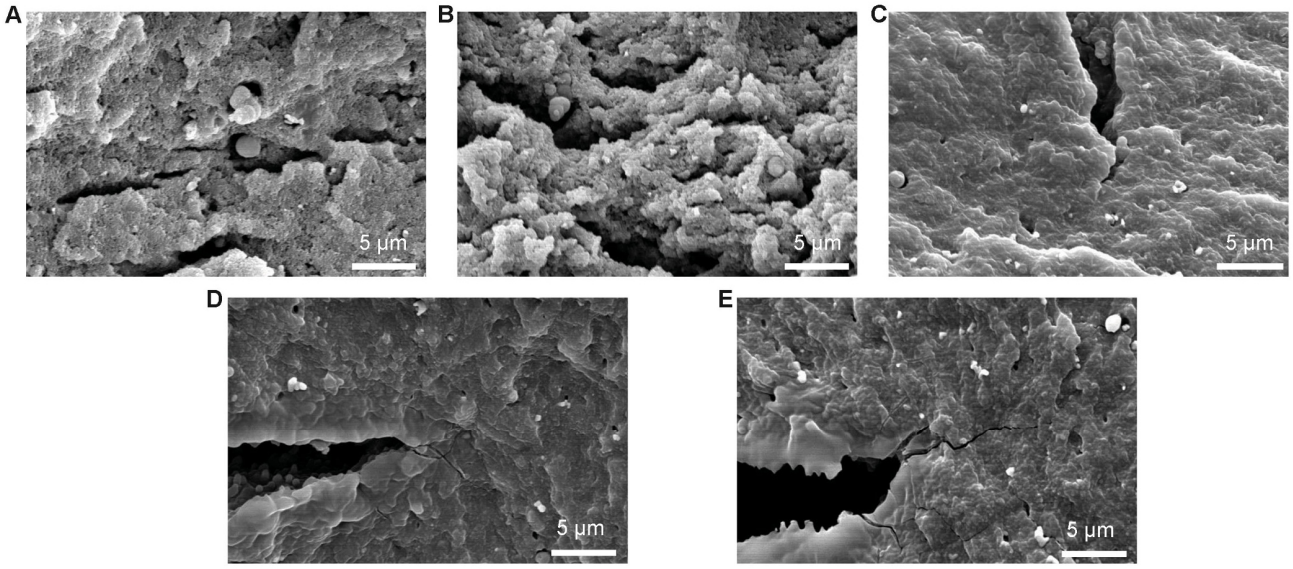

Fig. 5 SEM images of BMR/BR (100/0) (A), BMR/BR (90/10) (B), BMR/BR (50/50) (C), BMR/BR (10/90) (D) and BMR/BR (0/100) (E) rubber blends at 4000× magnifications

https://doi.org/10.1007/s40242-024-4001-0

to brittle fracture with increasing BR content.[9,28] Ductile and brittle fractures arise from distinct failure modes of crack initiation and propagation, respectively. This microscopic perspective further affirms that crack initiation primarily occurs before the threshold, whereas crack propagation becomes dominant afterward. Notably, when the blending ratio approaches the threshold, the mixture tends to form a double continuous interpenetrating network structure, reducing the likelihood of nano-cavitation formation and the speed of crack tip propagation. This inhibition of both crack initiation and propagation significantly enhances the fatigue life of the blend, contributing to the observed non-monotonic change in fatigue life.

4 Conclusions

In this study, a comprehensive investigation into the influence of crack initiation and propagation on the fatigue failure of BMR/BR binary blend rubber was conducted. The outcomes reveal a clear bifurcation in the dominant mechanisms driving fatigue failure based on the content of BR.

At lower BR content, the fatigue failure is predominantly instigated by crack initiation. This is substantiated by the observed rough and ductile fracture morphology in the SEM images, indicative of the propensity for microscopic crack formation under cyclic loading. Conversely, at higher BR content, the fatigue failure of the blend is primarily propelled by crack propagation. The shift to a smoother and brittle fracture surface further underscores the accelerated crack propagation rate, confirming the dominance of this mechanism after the threshold.

The critical observation emerges when BMR and BR contents are approximately equal, revealing a discernible threshold in the fatigue life of the blended rubber. Beyond this threshold, the fatigue life exhibits a diminishing trend. This pivotal insight not only offers a pathway for enhancing the fatigue properties of BMR but also provides a nuanced understanding of the interplay between crack initiation and propagation in the fatigue failure of BMR/BR blend rubber.

Furthermore, the implications of this study extend beyond BMR/BR blends, shedding light on fatigue failure mechanisms in NR/BR blends and other rubber formulations with a BR base. By unraveling the intricate dynamics of crack initiation and propagation, this research lays the groundwork for optimizing rubber blend formulations and advancing our comprehension of fatigue failure in diverse rubber composite systems.

Acknowledgements

This work was supported by the National Key R&D Program of China (No. 2022YFB3707303) and the National Natural Science Foundation of China (No. 52293471).

Conflicts of Interest

SUN Zhaoyan is a youth executive editorial board member for Chemical Research in Chinese Universities and was not involved in the editorial review or the decision to publish this article. The authors declare no conflicts of interest.

References

[1] Saad A. L. G., El-Sabbagh S., *Appl. Polym. Sci*., **2001**, *79*, 60
[2] Cao Y., Zhang J., Feng J., Wu P., *ACS Nano*, **2011**, *5*, 5920
[3] Shao H. F., Guo Q. R., He A. H., *Polym. Degrad. Stab*, **2021**, *191*, 109665
[4] Jovanovic S., Jovanovic S. S., Markovic G., Jovanovic V., Adamovic T., *Compos. B. Eng*., **2016**, *98*, 126
[5] Ghosh P., Stocek R., Gehde M., Mukhopadhyay R., Krishnakumar R., *Fract*., **2014**, *188*, 9
[6] Jurkowska B., Jurkowski B., Nadolny K., Krasnov A. P., Studniv Y. N., *Eur. Polym. J*., **2006**, *42*, 1676
[7] Wrana C., Schawe J. E. K., *Thermochimica Acta*, **2020**, *690*, 178699
[8] Kwag G., Kim P., Han S., Choi H., *Polymer,* **2005**, *46*, 3782
[9] Shangguan W. B., Wang X. L., Deng J. X., Rakheja S., Pan X. Y., Yu B., *Mater. Des*., **2014**, *58*, 65
[10] Le Cam J. B., Huneau B., Verron E., *Int. J. Fatigue*, **2013**, *52*, 82
[11] Gent A. N., Lindley P. B., Thomas A. G., *Appl. Polym. Sci.*, **1964**, *8*, 455
[12] Kwag G., Kim P., Han S., Lee S., Choi H., Kim S., *Appl. Polym. Sci*., **2007**, *105*, 477
[13] Kim H. J., Hamed G. R., *Rubber Chem. Technol*., **2000**, *73*, 743
[14] Lu Y. P., Wang Y. G., *Chinese J. Chem*., **2022**, *78*, 0518
[15] Mathew N. M., De S. K., *Int. J. Fatigue*, **1983**, *5* (1), 23
[16] Hess W. M., Vegvari P. C., Swor R. A., *Rubber Chem. Technol*, **1985**, *58* (2), 350
[17] Zaimova D., Bayrakta E. R., Miskioglu I., *Compos. B. Eng*., **2016**, *105*, 203
[18] Beatty J. R., *J. Elastomers Plast*., **1979**, *11* (2), 147
[19] Song Q., Wang F. F., Zhou S. F., Liu Y. Q., Zhao G. Z., *Syn. Mat. Aging and Application*, **2022**, *51* (2), 18
[20] Chiu H. T., Tsai P. A., *JMEPEG*, **2006**, *15*, 88
[21] Dong W., Fan W., Cui L., Dai Q., Bai C., *CN113861323A*, **2021**
[22] Fan W., He J., Dai Q., Bai C., *CN113929803A*, **2022**
[23] Bai C. X., He J. Y., Dai Q. Q., Qi Y. L., Cui L., *CN108409975-A*, **2018**
[24] Bhattacharya M., Bhowmick A. K., *J. Mater. Sci*., **2010**, *45*, 6139
[25] Qiu X. W., Yin H. S., Xing Q. C., *J. Polymers*, **2022**, *14*, 4592
[26] Tee Y. L., Loo M. S., Andriyana A., *Int. J. Fatigue*, **2018**, *110*, 115
[27] Xiong S. F., Liu J., Zhou J. K., Lei W. W., *Polym. Bull.*, **2023**, *36* (5), 574
[28] Pal P. K., Bhowmick A. K., De S. K., *Int. J. Polym. Mater.*, **1982**, *9* (2), 139
[29] Bakhshizade A., Ghalebahman A. G., Hajimousa M. A., *Adv. Polym.*, **2022**, *22*, 5950215